Chondrites and the Protoplanetary Disk
ASP Conference Series, Vol. 341, 2005
A. N. Krot, E. R. D. Scott, & B. Reipurth, eds.

Photochemical Speciation of Oxygen Isotopes in the Solar Nebula

J. R. Lyons and E. D. Young

Department of Earth and Space Sciences, University of California, 595 Charles Young Dr. East, Los Angeles, California 90095-1567, USA

Abstract. We have performed time-dependent photochemical calculations of CO self-shielding in the surface region of a turbulent nebula, and demonstrated that substantial mass-independent fractionation in bulk oxygen isotopes in the nebula was possible on timescales of 10^5 years. CO photodissociation in the presence of abundant H_2 yields δ-values for nebular H_2O with $\delta^{17}O/\delta^{18}O$ near 1.0, consistent with measurements in Ca-Al-rich inclusions. This mechanism provides a self-consistent explanation for the oxygen isotope values of nebular water inferred from secondary minerals in unequilibrated chondrites, and places constraints on the far-ultraviolet radiation in the solar nebula environment and the strength of turbulent vertical mixing in the nebula.

1. Introduction

The three isotopes of oxygen (^{16}O, ^{17}O, and ^{18}O) occupy a special place in stable isotope studies of terrestrial and extraterrestrial materials. The large elemental abundance of oxygen and its simultaneous occurrence in both gas and solid phases under a wide range of pressures and temperatures mean that oxygen isotopes provide a record of numerous fractionation processes in various environments. Because oxygen has three isotopes, comparison of multiple isotope ratios ($^{18}O/^{16}O$ and $^{17}O/^{16}O$) allows for unambiguous identification of anomalous isotope chemistry. Here, we present a quantitative model for anomalous isotope fractionation in the solar nebula due to photolysis of CO.

Highly refractory calcium-aluminum-rich inclusions (CAIs) in primitive meteorites (chondrites) were the first natural materials discovered with large anomalous oxygen isotope ratios (Clayton, Grossman, & Mayeda 1973). In isotopically equilibrated materials, the fractionation of $^{17}O/^{16}O$ (relative to a reference material) is approximately one half (0.52) that of $^{18}O/^{16}O$, and is referred to as 'mass-dependent' fractionation. The factor of 0.52 arises from the difference in vibrational energies of normal and isotope substituted molecules (Matsuhisa et al. 1978). In CAIs, Clayton et al. (1973) discovered that $^{17}O/^{16}O$ and $^{18}O/^{16}O$ were fractionated by nearly equal amounts, and described the oxygen isotopes as being 'non-mass-dependently' (or 'mass-independently') fractionated. This remarkable discovery has stimulated work on many radiogenic, chemical and photochemical isotope anomalies in both terrestrial and non-terrestrial materials.

Figure 1 shows oxygen isotope data collected for bulk CAIs (Clayton et al. 1977; see also references in McKeegan & Leshin 2001) as well as by laser ablation analysis of individual CAI minerals (Young & Russell 1998). Oxygen isotope ratios are displayed as δ-values, where

$$\delta^{x}O_{SMOW}(u) = 10^{3}\left(\frac{(^{x}O/^{16}O)_{u}}{(^{x}O/^{16}O)_{SMOW}} - 1\right) \qquad (1)$$

for x = 17 or 18, and SMOW is 'Standard Mean Ocean Water'. The data of Clayton and colleagues defined a line of slope = 0.94 on the plot of $\delta^{17}O$ vs. $\delta^{18}O$, which they defined as the 'carbonaceous chondrite anhydrous mineral' (CCAM) line. More recent laser ablation analyses on CAIs in the Allende meteorite (Young & Russell 1998) see evidence for a line of slope = 1.00. Clayton et al. (1977) interpreted the CCAM line as a mixing line between nebular solids enriched in ^{16}O and nebular gas depleted in ^{16}O. The minimum initial nebular water δ-values inferred from the Murchison meteorite (Clayton & Mayeda 1984; Young 2001) are also shown (Fig. 1). Supernova input of pure ^{16}O into the solar nebula was originally believed to be the source of ^{16}O enrichment, but the lack of similar fractionation in other elements argues against this scenario (Clayton 1993). The mechanism of ^{16}O depletion in the gas was unknown.

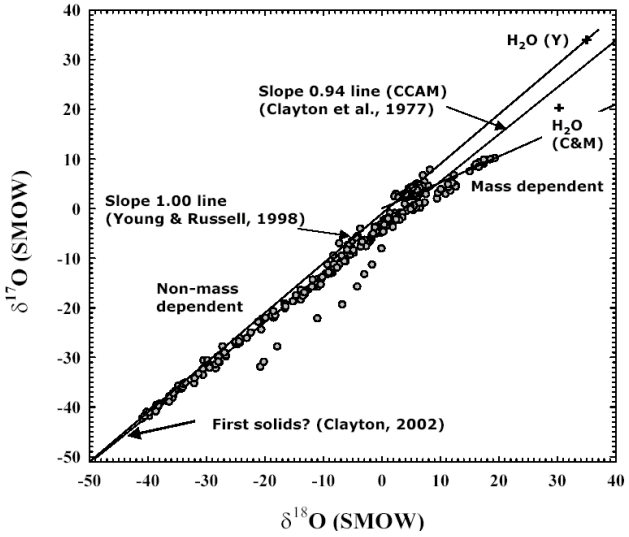

Figure 1. Oxygen isotope compositions of CAIs. Data are high precision bulk and mineral separate analyses from the laboratory of R. Clayton (e.g., Clayton et al. 1977; see also references in McKeegan & Leshin 2001), and laser-ablation data from E. Young (e.g., Young & Russell 1998). The CAI mixing line discovered by Clayton and colleagues (Clayton et al. 1973) is indicated as 'CCAM' and has a slope of about 0.94. Laser ablation data on several Allende CAIs shows evidence for a mixing line of slope = 1.00. The two H_2O points ('Y' and 'C & M') are initial nebular water (liquid) values inferred from the Murchison meteorite.

Oxygen isotope analyses have also been performed for each meteorite group. Figure 2 (McKeegan & Leshin 2001) shows $\Delta^{17}O$ versus $\delta^{18}O$ for whole rock chondrites (data are mostly from the laboratory of R. Clayton). $\Delta^{17}O$ is a measure of mass-independent fractionation (MIF) and is defined as $\Delta^{17}O = \delta^{17}O - 0.52 \times \delta^{18}O$. Each meteorite group defines a specific, although not completely unique, field on this plot, suggesting that oxygen isotopes are correlated with different meteorite groups. SNC meteorites (not shown) also define a unique field with $\Delta^{17}O$ = 0.3‰ and $\delta^{18}O$ of about 4 – 5‰, between the ordinary chondrites and enstatite chondrites.

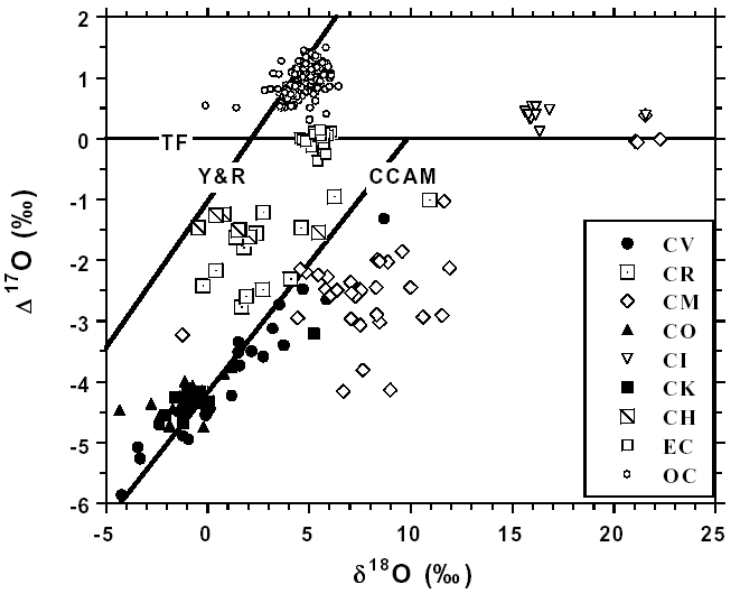

Figure 2. Oxygen isotope compositions of whole-rock chondrites according to group. Most of the data shown are from the laboratory of R. Clayton (see McKeegan & Leshin 2001 for references). Error bars are similar to symbol sizes. Each meteorite group occupies a distinct or nearly distinct field on this diagram. The CCAM and slope 1.0 (Y & R) lines are also shown. (Figure from McKeegan & Leshin 2001).

Our purpose here is not to explore the full complexity of Figure 2, but rather to understand the origin of the ^{16}O depleted gas reservoir shown in Figure 1. Previous attempts to explain the CAI mixing line include a proposed chemical MIF mechanism, analogous to that during ozone (O_3) formation (Thiemens & Heidenreich 1983; Gao & Marcus 2001). Although ozone is not likely to have been an important component of the solar nebula, Marcus (2004) has proposed that gas-grain silicate reactions in the inner solar nebula may have produced a chemical MIF. However, experimental evidence for MIF in such reactions is lacking. It has also been suggested that production of ^{17}O and ^{18}O in AGB stars enriched the gas in the interstellar medium relative to dust over time (Clayton 1988).

Recently, it was suggested (Clayton 2002) that self-shielding of CO during photolysis reactions in the innermost solar nebula (adjacent to the X-point) produced the MIF. The possibility of CO self-shielding in the nebula was recognized by Thiemens & Heidenreich (1983) and by Navon & Wasserburg (1985), but these authors did not quantify the process, nor did they infer the implications for solar oxygen isotopes. Because CO photodissociates by line absorption, the most abundant isotopologue ($C^{16}O$) saturates, and dissociation of less abundant $C^{18}O$ and $C^{17}O$ produces a zone of enrichment of ^{18}O and ^{17}O (Fig. 3). High temperature reactions of O with H_2 rapidly produce ^{16}O-depleted H_2O, thus forming the initial nebular water reservoir inferred from unequilibrated meteorites (Fig. 1). Clayton (2002) then hypothesized that high temperature reaction of H_2O with ^{16}O-enriched dust produced the measured CAI mixing line. In order to get the altered silicates into the terrestrial planet forming region of the solar nebula, Clayton (2002) invoked transport from the X-point region by the X-wind to the 1 – 3 AU region. A key implication of Clayton's self-shielding scenario is that solar oxygen isotopes are similar to the lightest CAIs. A full quantitative assessment of X-point self-shielding scenario has yet to be performed, but at least three difficulties exist. First, CO self-shielding is almost certainly less effective at high temperatures due to greatly enhanced band and line overlap (Navon & Wasserburg 1985). Second, absorption by H_2O would reduce the depth of UV radiation into the nebula. Third, high temperatures in this region would have rapidly erased the MIF signature by reactions of carbon atoms with H_2O (Lyons & Young 2003).

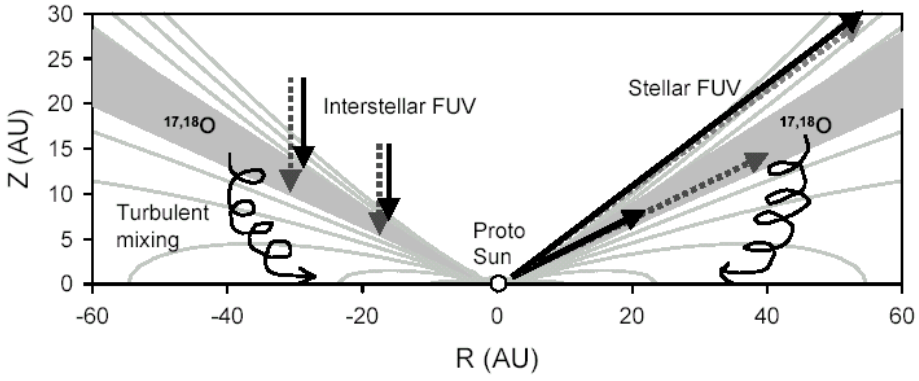

Figure 3. Schematic diagram of CO self-shielding at the disk surface due to interstellar radiation normal to the disk and radiation from the central star. The contours indicate decades in gas density. Saturation of $C^{16}O$ absorption lines results in ^{17}O and ^{18}O enhancement at the disk surface (shaded region). Here we consider only interstellar radiation.

Although we believe that CO self-shielding in the innermost solar nebula is problematic, we agree with Clayton (2002) that photochemical processes are the source of the ^{16}O-depleted reservoir. Here, we report time-dependent photochemical calculations of CO self-shielding in the cooler, surface region of a turbulent nebula, and demonstrate that substantial MIF in bulk oxygen isotopes in the nebula was possible on timescales of 10^5 years. This mechanism provides a self-consistent explanation for the oxygen isotope values of nebular water inferred from secondary minerals in unequilibrated chondrites (Clayton & Mayeda 1984; Choi et al. 1998; Young 2001), and places constraints on key nebula parameters.

The CO self-shielding mechanism is attractive as an explanation for the isotope anomaly in CAIs because it invokes a process known to occur in CO in molecular clouds (Bally & Langer 1982; van Dishoeck & Black 1988; Sheffer, Lambert, & Federman 2002), and because it naturally yields nearly mass-independent oxygen isotope fractionation. Very large fractionations (10^4 ‰) are predicted (van Dishoeck & Black 1988) and observed (Sheffer et al. 2002; Federman et al. 2003) in diffuse and translucent molecular clouds, and it has recently been suggested (Yurimoto & Kuramoto 2004) that H_2O produced by CO dissociation in the parent molecular cloud can explain oxygen isotopes in CAIs. Because large oxygen isotope fractionations are not observed in cloud cores, e.g., $^{16}O/^{18}O \sim 500$ and $^{16}O/^{17}O \sim 2600$ in the solar neighborhood (Federman et al. 2003), this mechanism implies that the solar nebula may have derived from mixing of a small amount of cloud envelope material with an unfractionated core. Star formation results from core collapse in dense molecular clouds, and it is unclear whether large fractionations in more tenuous clouds are inherited by protostellar nebulae. Nor is it known to what extent cloud cores inherit oxygen isotope fractionation from their diffuse and translucent cloud precursors. Because the uncertainties in the astronomical oxygen isotope ratios are considerably larger than the 5% difference between the lightest CAIs and bulk Earth (Federman et al. 2003), it is not yet possible to accurately describe oxygen isotope reservoirs in molecular clouds.

2. Solar Nebula Model

2.1. Disk Model

Surface regions of the nebula are similar in temperature and pressure to dense molecular clouds and are therefore another likely site for formation and preservation of oxygen isotope heterogeneity as a result of self-shielding (Lyons 2002; Young & Lyons 2003). To investigate the influence of CO self-shielding on oxygen isotope ratios in the early solar system, we employed a one-dimensional photochemical model to compute the time-dependent oxygen isotope profiles in a two-dimensional, axisymmetric nebula (Lyons & Young 2004; Lyons & Young 2005). The total gas number density in the disk was specified with a standard analytical disk model (Aikawa & Herbst 2001). For a nebula of bulk composition similar to solar (Anders & Grevesse 1989; Allende Prieto, Lambert, & Asplund 2002), the initial volume fractions are $f_{He} = 0.16$, $f_{CO} = 2 \times 10^{-4}$, $f_{H2O} = 2 \times 10^{-4}$, and $f_{MgFeSiO4} = 2 \times 10^{-5}$, assuming all C is in CO, all Si is in $MgFeSiO_4$, and all remaining O is in H_2O.

2.2. Photochemical Model

Disk photochemistry in the model is initiated by CO photodissociation from 91.2 to 110 nm,

$$C^xO + h\nu \rightarrow C + {}^xO \qquad (2)$$

where x = 16, 17, and 18, and by H_2 and H photoionization at wavelengths shortward of 91.2 nm. Disk chemistry was restricted to H, C, and O-containing chemical species, and the reaction rate coefficients used are a subset of the UMIST database (Le Teuff, Millar, & Markwick 2000). By utilizing previously published disk models (Hasegawa, Herbst, & Leung 1992; Willacy et al. 1998; D'Alessio et al. 1999; Aikawa & Herbst 2001; Aikawa et al. 2002), we developed a reduced set of 96 species and 375 reactions to model the disk chemistry. Gas-grain reactions are also included using published desorption energies (Hasegawa et al. 1992; Willacy et al. 1998). Although our model is less sophisticated in its treatment of chemistry and radiative transfer than some recent models (Markwick et al. 2002; van Zadelhoff et al. 2003), it is the first model to include both vertical transport and oxygen isotopes.

To follow the time evolution and vertical distribution of O-containing species in the disk resulting from CO photodissociation high above the midplane, we solved the one-dimensional continuity equation for each species as a function of height *z* above the midplane:

$$\frac{\partial f_i}{\partial t} = \frac{1}{n}\frac{\partial}{\partial z}\left(D_v n \frac{\partial f_i}{\partial z}\right) + \frac{P_i}{n} - L_i f_i \qquad (3)$$

where f_i is the volume fraction of species *i*, *n* is the number density of the background gas (H_2 and He), and *t* is time measured from the initiation of FUV radiation on the disk. Vertical motion is characterized by a vertical eddy diffusion coefficient, D_v, which is assumed here to be comparable to the turbulent viscosity, $\nu_t = \alpha c H$, where c is the sound speed, *H* is the vertical scale height in the nebular gas, and $\alpha < 1$ is a parameter commonly used in disk models to describe the strength of turbulent mixing (Stone et al. 2000). Arguments have been made for $D_v < \nu_t$ (Stevenson 1990) and $D_v > \nu_t$ (Prinn 1990). P_i and L_i are the production rate (molecules cm^{-3} s^{-1}) and loss frequency (molecules s^{-1}), respectively, for each species in the model. The initial abundance ratios of the CO isotopologues are assumed to be approximately terrestrial with values of 500 and 2600 for $^{12}C^{16}O/^{12}C^{18}O$ and $^{12}C^{16}O/^{12}C^{17}O$, respectively. All quantities depend on *r*, the radial location in the disk, and so a value of *r* must be specified. We have chosen *r* = 30 AU as representative of cold regions of the disk where water ice formation is expected. The midplane temperature is 51 K at 30 AU. Calculations at smaller heliocentric distances (higher temperatures) are in progress. Water has a significant vapor fraction at temperatures > 120 K.

Photodissociation of CO isotopologues must account for self-absorption of a given isotopologue (i.e., self-shielding) and overlap of different isotopologue spectra (i.e., mutual-shielding). To quantify the effects of self and mutual-shielding, we derived fits to the results of van Dishoeck & Black (1988) and Lee et al. (1996) devel-

oped for molecular clouds in the interstellar medium. [A more detailed discussion of shielding functions is given in Lyons & Young (2005)]. Photodissociation of each CO isotopologue is proportional to the product εJ_{ISM}, where $J_{ISM} = 2.0 \times 10^{-10}$ s^{-1} is the rate constant for CO photolysis due to the interstellar medium (ISM) UV field (van Dishoeck & Black 1988), and ε is a FUV flux enhancement factor. Dust opacity is identical for all isotopologues, and was parameterized in the same manner as is done for the interstellar medium (Kamp & Bertoldi 2000). We consider a FUV range of $\varepsilon = 1$ to 10^5, the upper end of which is consistent with FUV-enhancements in pre-main sequence stars (Imhoff & Appenzeller 1987), and also with proximity to a massive O star in a star-forming region.

2.3. Isotope Calculations

The oxygen isotope composition of species in the nebula was computed using equation (1), but relative to initial CO in the nebula rather than to SMOW. Initial CO was assumed to have oxygen isotope ratios of $^{16}O/^{18}O = 500$ and $^{16}O/^{17}O = 2600$. The shift in isotopic composition for an unknown 'u' from a 'CO initial' reference to a standard mean ocean water ('SMOW') reference is given by

$$\delta^x O_{SMOW}(u) = \delta^x O_{CO_{initial}}(u) + \delta^x O_{SMOW}(CO_{initial}) + 10^{-3}\delta^x O_{CO_{initial}}(u)\delta^x O_{SMOW}(u) \quad (4)$$

where x = 17 or 18, and $\delta^x O_{SMOW(CO_{initial})} = -50‰$. The oxygen isotope composition of total nebular H_2O is then given by

$$\delta^x O_{SMOW}(H_2O_{tot}) = \frac{f_{H_2O_{cloud}}\delta^x O_{SMOW}(H_2O_{cloud}) + f_{H_2O_{ss}}(t)\delta^x O_{SMOW}(H_2O_{ss})}{f_{H_2O_{cloud}} + f_{H_2O_{ss}}(t)} \quad (5)$$

where the volume fraction of H_2O from the parent cloud is $f_{H2O\ cloud} = 2 \times 10^{-4}$, the isotope composition of the H_2O in the cloud is $\delta^x O_{SMOW(H_2O_{initial})} = -50‰$, $f_{H2O}(t)$ is the volume fraction of H_2O produced from CO photodissociation (H_2O_{ss}) , and $x = 17$ or 18.

3. Results

Integration of the system of continuity equations yields the time evolution of species volume fractions in the model. Figure 4a shows results from 10^3 to 10^7 years for r = 30 AU in the disk midplane. We assumed $\alpha = 10^{-2}$, consistent with previously published estimates (Stone et al. 2000; Cuzzi, Dobrovolskis, & Hogan 1996), and ε = 500; the latter implies a dust temperature of 110 K at the disk surface. Following CO and H_2 dissociation in the model, H_2O is formed via reactions between H and O on grain surfaces (H_2O_{ss}); C is ionized and forms a suite of hydrocarbon ions and molecules (not shown) as is predicted in other disk models (e.g., Willacy et al. 1998). The formation timescale for H_2O is 10^5 years at the midplane at 30 AU. The timescales for dissociation of CO and formation of H_2O become longer at smaller heliocentric distances due to the larger vertical column abundance of gas. Figure 4b shows the model delta-values of CO and H_2O_{ss} isotopologues at the midplane, assuming initial values of -50‰ for both $\delta^{17}O$ and $\delta^{18}O$ for CO and H_2O from the parent molecular

cloud. Water in the nebula consists of H_2O from the parent molecular cloud and the H_2O produced via CO self-shielding. We assumed that CO and H_2O from the parent cloud had oxygen isotope values similar to the isotopically lightest CAIs with $\delta^{17}O_{SMOW} = \delta^{18}O_{SMOW} = -50‰$, as suggested by Clayton (2002). A key prediction of the model presented here and the molecular cloud self-shielding model (Yurimoto & Kuramoto 2004) is that CO in the outer solar system is isotopically very light, $\delta^{18}O_{SMOW}(CO) \sim -200‰$ to $-500‰$.

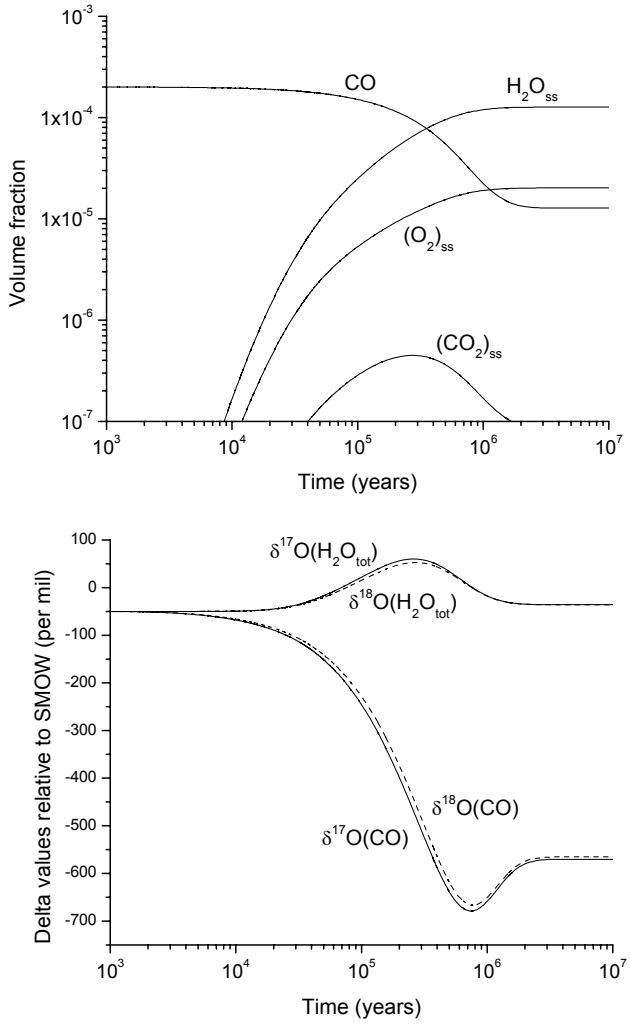

Figure 4. a (top) - Time-dependent model results at the disk midplane for r = 30 AU, $T_{midplane}$ = 51K, $\alpha = 10^{-2}$, and 0.1 μm dust particles. The FUV flux enhancement factor ε = 500 times the ISM FUV flux. Volume fractions of several species relative to total nebular gas. H_2O_{ss} and $(CO_2)_{ss}$ were produced as a result of CO photodissociation. b (bottom) - As in Figure 4a, $\delta^{17}O$ and $\delta^{18}O$ of CO and total nebular H_2O relative to SMOW. (From Lyons & Young 2005).

Figure 5 shows the time evolution of the mass-independent oxygen isotope component $\Delta^{17}O_{SMOW}$ of the isotopic composition of total nebular H_2O for several values of FUV flux. For $\varepsilon = 5$, 50, and 500, $\Delta^{17}O_{SMOW}$ (H_2O) values at the midplane are within or above estimates of the minimum $\Delta^{17}O_{SMOW}$ for initial H_2O in the solar nebula (Clayton & Mayeda 1984; Choi et al. 1998; Young 2001). Lower FUV fluxes do not photolyze enough CO within 1 Myr to produce sufficient fractionation at the midplane. For a given α the maximum $\Delta^{17}O_{SMOW}$ (H_2O) decreases as FUV flux increases due to increased photolysis of $C^{16}O$, suggesting that it may be possible to place an upper limit on the FUV incident upon the disk. The isotopic composition of nebular H_2O is also dependent on α. Results for $\alpha = 10^{-3}$ (not shown) are similar to $\alpha = 10^{-2}$, but timescales are about 3 times longer. For $\alpha = 10^{-4}$ weak mixing implies an insufficient turnover of CO to maintain efficient self-shielding, yielding $\Delta^{17}O_{SMOW}$ (H_2O) well below the values inferred from meteorites. Thus, the value of $\Delta^{17}O_{SMOW}$ of nebular H_2O predicted by the model for a distance of 30 AU is sensitive to a key disk parameter, α, and to a key nebular environment parameter, the FUV flux incident on the disk. Preliminary results at smaller heliocentric distances are similar but the timescales become longer. At 10 AU $\Delta^{17}O_{SMOW}$ of nebular H_2O at the midplane reaches a maximum in ~ 10^6 years.

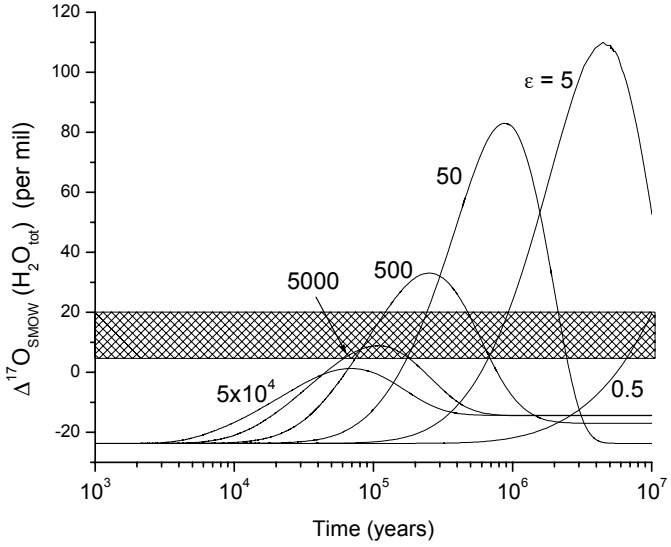

Figure 5. The mass-independent fractionation (relative to SMOW) of total H_2O in the nebula midplane for $\alpha = 10^{-2}$, various FUV flux enhancement factors, and 0.1 μm particles. The shaded area indicates the range of minimum $\Delta^{17}O_{SMOW}$ inferred for initial nebular H_2O from analyses of carbonaceous chondrites (Clayton & Mayeda 1984; Young 2001); higher $\Delta^{17}O_{SMOW}$ values of initial nebula water are allowed by the meteorite data. (Figure from Lyons & Young 2005).

Figure 6 shows the trajectory of $\delta^{17}O_{SMOW}$ and $\delta^{18}O_{SMOW}$ values of nebular water at the midplane for $\varepsilon = 500$. The slope of the trajectory is about 10% too high compared to the slope-0.94 line (Clayton 1993), and about 5% higher than the slope-1.0 line (Young & Russell 1998). A similar slope was estimated (Navon & Wasserberg 1985) for self-shielding in pure O_2. A slope > 1 is expected for pure CO because of the greater abundance, and therefore greater self-shielding, of $C^{18}O$ compared to $C^{17}O$. In a nebula, CO dissociation occurs in an H_2-rich environment, and H_2 absorption must be accounted for. van Dishoeck & Black (1988) showed that approximately 50% of the dissociation of $C^{18}O$ in molecular clouds occurs in a particular band of CO (band #31). Figure 7 demonstrates that inclusion of band #31, using the H_2 synthetic spectra of McCandliss (2003) brings the model slope into better agreement with inferred nebular water. This analysis applies to both the outer region of the disk discussed here, and to the parent molecular cloud. Because the cloud model of Maréchal, Viala, & Pagani (1997) did not include ^{17}O, Yurimoto & Kuramoto (2004) could not quantitatively address the $\delta^{17}O/\delta^{18}O$ ratio expected from CO self-shielding, and thus could not test an essential aspect of the self-shielding theory.

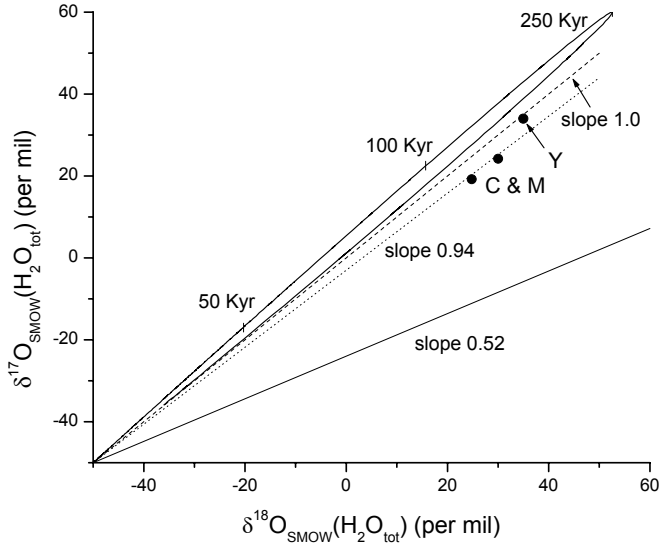

Figure 6. Three-isotope plot ($\delta^{17}O$ vs. $\delta^{18}O$) for total nebular H_2O for $\alpha = 10^{-2}$ and 0.1 μm dust. Results are shown for $\varepsilon = 500$ with time labelled along the trajectory. Lines of slope 1.0 (Young & Russell 1998), slope 0.94 (the carbonaceous chondrite anhydrous mineral, or CCAM, line from Clayton et al. (1973)), and slope 0.52 (a mass-dependent fractionation line) are shown for reference. The minimum isotopic composition of initial nebular H_2O, as inferred from analyses of carbonaceous chondrites, is indicated by 'C & M' (Clayton & Mayeda 1984) and 'Y' (Young 2001). The 'C & M' value is for initial nebular gas, and the 'Y' value is for initial nebular liquid water. (Figure from Lyons & Young 2005).

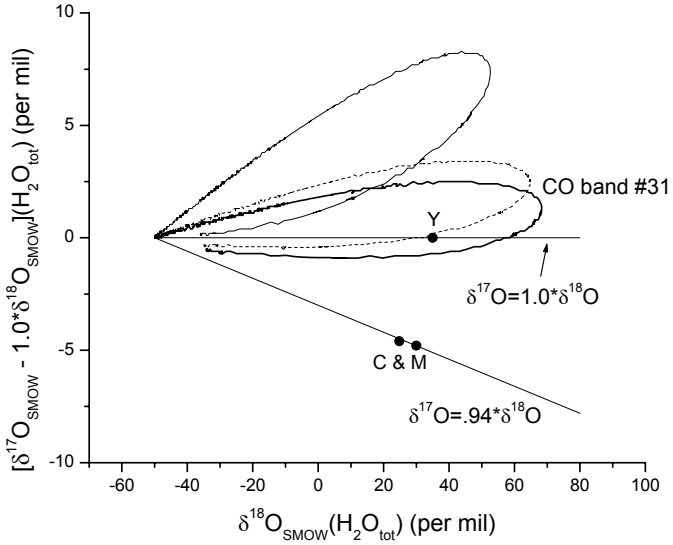

Figure 7. Three-isotope plot of total nebular H_2O but with the ordinate transformed from $\delta^{18}O$ to $\delta^{17}O - 1.0 \times \delta^{18}O$. The unlabeled curve is the same as the trajectory shown in Figure 6. The solid red curve includes differential mutual shielding by H_2 on CO band number 31, which brings the model isotope fractionation close to the measured range in CAIs (Clayton et al. 1973; Clayton & Mayeda 1984; Young & Russell 1998). The effect of differential shielding corresponding to an H_2 column density of 1.5×10^{21} cm^{-2} is also shown (dotted line). (Figure from Lyons & Young 2005).

4. Comparison of Nebular Self-Shielding and Nebular Inheritance of Parent Cloud Self-Shielding

Here we compare timescales for the two self-shielding scenarios, nebular self-shielding and nebular inheritance of parent cloud self-shielding, and discuss some additional chemical processes that must be considered in the parent cloud scenario. In the case of nebular H_2O from O. Reformation of CO by various reactions in the nebular model (Lyons & Young 2005) means that $t_{CO} > J_{CO}^{-1}$, where J_{CO} is the photolysis rate constant for CO in the FUV active zone (Lyons & Young 2004). The radial and vertical mixing timescales in the nebula are $t_r \sim r^2/D_v \sim r^2/\alpha cH$ and $t_v \sim H/\alpha c$, which at $r = 30$ AU and $\alpha = 10^{-2}$ are $t_r \sim 10^5$ years and $t_v \sim 10^3$ years. Lyons & Young (2005) showed that at 30 AU and for a FUV flux ~ 10^3 times the local ISM (LISM) $t_{CO} \sim 10^5$ years. For a spatially uniform FUV flux t_{CO} increases with decreasing heliocentric distance due to the higher vertical column density of gas at smaller r, so that at 10 AU $t_{CO} \sim 10^6$ years. Observations of protoplanetary disks suggest a residence time for the gas of the order of several million years. Thus, for a FUV flux ~ 10^3 times LISM, as would be expected for a stellar association of several hundred stars (Adams et al. 2004), nebular self-shielding would not be important for $r <$ 5-10 AU.

However, because $t_{CO} \sim t_r$ at 30 AU, CO photolysis and inward radial transport may have supplied the inner solar with the necessary oxygen isotope anomaly. FUV radiation from the protosun, which varies as r^{-2}, would have decreased J_{CO}, but this depends highly on the disk geometry. For a line-of-sight angle with the FUV surface of the disk of ~ 0.1 radians, and a 10^3-fold enhancement in the protosolar FUV flux (Imhoff & Appenzeller 1987), the principal FUV source for $r < 30$ AU was the protosun, while for $r > 30$ AU the principal FUV source would be the 10^3-fold enhancement in ISM FUV assumed in Lyons & Young (2005). For FUV fluxes >> $10^3 \times$ LISM, very high gas temperatures and disk photoevaporation occur (Adams et al. 2004), neither of which has been accounted for in the Lyons & Young (2005) model.

Because H_2O formation occurs primarily on grain surfaces and because the principal source of FUV absorption is dust in the Lyons & Young (2005) model, the timescales for dust growth and settling must also be considered. Dust was assumed to be 0.1 microns in size and uniformly distributed in the disk, and grain growth and settling were neglected. Grain collisions by Brownian motion occur on a timescale $t_{coll} \sim 10^2$ years at the midplane at 30 AU; in the FUV surface $t_{coll} \sim 10^4$-10^5 years. At the midplane the particle friction time (i.e., the response time of the particles to gas drag) is $t_f \sim r_p \rho_p / c \rho_g \sim 10^3$ seconds, where r_p and ρ_p are the particle radius and density, and ρ_g is the gas density. The inner timescale of turbulence (i.e., the turnover time of the smallest turbulent eddies) is $t_i \sim t_K (\nu_m / \nu_t)^{0.5} \sim 10^6$ seconds, where t_K is the Keplerian orbital period, and ν_m is the molecular viscosity (Cuzzi, Dobrovolskis, & Hogan 1996). Because $t_f << t_i$, turbulent particle growth can be neglected. Dust settling timescales are ~ 10^5 years in the midplane and ~ 10^3 years in the FUV zone (Chiang & Goldreich 1997), but dust coupling to vertical gas motions will increase these timescales. The relative velocity due to Brownian motion of colliding dust grains is ~ 2 cm s^{-1} at 30 AU (50 K midplane temperature), so the sticking efficiency of colliding particles should be near unity (Wurm & Blum 1998). Thus, at 30 AU dust particles in the Lyons & Young (2005) model will be mostly entrained in the gas and will be vertically transported on a 10^3-year timescale, but particle loss will likely occur near the midplane. Particles that grow on timescales < 10^4 years will probably not incorporate a significant amount of anomalously fractionated water ice produced by nebular self-shielding. However, because the decrease in dust particle concentration will increase the rate of CO photolysis, the overall effect of dust growth is not obvious. Clearly, dust growth must be included in future versions of the nebular self-shielding model.

In the nebular inheritance model of Yurimoto & Kuramoto (2004), anomalously fractionated H_2O is formed as a result of CO self-shielding and condensed onto dust grains within the parent cloud. The timescales on which this occurs can be the age of the cloud (~ 1-10 Myr). The amount of H_2O produced as a result of CO photodissociation will depend on the FUV flux in the vicinity of the cloud and also on turbulent mixing within the cloud. Yurimoto and Kuramoto (2004) utilized results from a molecular cloud model (Marechal, Viala, & Pagani 1997) that accounted for self-shielding in $C^{16}O$ and tracked ^{18}O and ^{16}O into various other species (e.g., O_2, OH, H_2O). The purpose of the Marechal et al. (1997) model was to predict $^{16}O^{18}O$ distribution in molecular clouds for comparison with observational upper limits. Marechal et al. (1997) considered a range of FUV fluxes but did not consider cloud mixing. Using the Marechal et al. (1997) results for $H_2{}^{16}O$ and $H_2{}^{18}O$ (^{17}O was not included in the cloud model) formed by ion-molecule reactions initiated by the reaction of O^+

with H_2, Yurimoto & Kuramoto (2004) showed that H_2O produced from O liberated during CO self-shielding could yield a bulk nebular oxygen isotope anomaly large enough to explain the CAI mixing line. Key to the Yurimoto & Kuramoto (2004) model, as well as to the nebular self-shielding model (Lyons & Young 2005), is concentration of H_2O at the nebula midplane, most likely as ice-coated dust particles.

A roughly solar mass core within the cloud collapses on timescales of ~ 10^5 years. As a disk and central mass form, subsequently accreted gas and dust pass through an accretion shock as the material infall velocity, v_{in}, is reduced to the thermal speed of the nebular gas. For a nearly solar mass central object the median shock velocity is ~ 17, 7.7 and 3.1 km s^{-1} at disk radii of 1, 5 and 30 AU, respectively (Cassen & Moosman 1981). The corresponding temperatures behind the shock front are 15000, 3100, and 500 K (Neufeld & Hollenbach 1994). Rapid chemical and isotopic processing will occur in the gas at temperatures > 1500-2000 K. In the cloud model of Marechal et al. (1997), the principal O-containing species are O, CO, OH, O_2, and H_2O. CO has a negative isotope ($\Delta^{17}O<0$) relative to bulk cloud O; the other O-containing species have positive isotope anomalies. When the accreting gas is shock heated a number of chemical processes may occur, including isotope exchange between O and CO, O and O_2, and OH and H_2O. Additionally, water will be formed by high-temperature reactions of O, OH and O_2 with H_2. Depending on the relative rates of reaction of the various oxygen isotope exchange reactions with H_2O formation reactions, both the fraction and isotopic composition of gas-phase water in the shocked gas may be quite different from the parent cloud gas. One of us (JRL) is presently investigating the isotopic consequences of shock heating during accretion of the parent cloud gas.

Dust particles are much less affected by the accretion shock. Because the particles are not well coupled to the gas, they pass through the shock front and are heated by gas drag beyond the shock front (Chick & Cassen 1997; Lunine et al. 1991). Maximum dust heating occurs at a gas density $n \sim 10^{11}$–10^{12} cm^{-3}, which corresponds to the midplane gas density at 30 AU for the Lyons and Young (2005) disk model. Thus, evaporated water is deposited ~ 3 scale heights below the FUV surface region of the disk, which will protect the gas-phase water from rapid photolysis. (For a 10^3-fold enhancement over LISM FUV, H_2O is photolyzed in < 1 year in the FUV active zone.) Thus, the important timescales are the cooling time for the shocked gas, t_{cool}, the condensation time, t_{cond}, for gas-phase H_2O to recondense onto dust grains, and the vertical mixing time, t_v. Using the thermal timescale of Chiang & Goldreich (1997), $t_{cool} \sim 1$–10 years at 30 AU. At the midplane of the Lyons & Young model $t_{cond} \sim 10^6$ seconds = 0.025 years, assuming a gas temperature < 120 K, the condensation temperature of water. Thus both t_{cool} and $t_{cond} << t_v \sim 10^3$ years, and much of the water evaporated during passage of ice-coated dust particles through the accretion shock will recondense onto dust particles before either photolysis or oxygen isotope exchange can occur (Lunine et al. 1991). For water vapor that makes it to the FUV active zone, photolysis rapidly produces O_2, which cannot be concentrated in the disk midplane by condensation onto grains. This limits direct input of parent cloud water ice to regions of the disk with T < 120 K, or disk radii > 5 AU for the disk model assumed here. The timescales for formation of an anomalously fractionated ice reservoir by nebular inheritance from the parent cloud are considerably shorter than t_{CO} in

the nebular self-shielding model, which favors the nebular inheritance model but does not preclude a contribution from nebular self-shielding.

Chemical and isotopic processing of parent cloud gas in the accretion shock could either reinforce or alter this conclusion. If the shocked gas forms considerable additional H_2O with $\Delta^{17}O > 0$ before exchange reactions can erase the anomalous fractionation, then the water ice contribution from grains may simply represent a small additional reservoir of anomalous oxygen. Alternatively, if the shocked gas forms a large water reservoir with zero or very small anomalous fractionation (due to isotopic exchange with CO at high temperatures), then the water-ice contribution from dust particles maybe insufficient to account for the CAI mixing line. Both of these possibilities must be evaluated with additional chemical modeling and astronomical observations.

5. Radial Transport of Nebular Water

Transfer of the MIF signature in nebular water to the rocky component of the nebula requires that H_2O must have been concentrated relative to CO in the disk midplane (Yurimoto & Kuramoto 2004). Without concentration of H_2O at the midplane, equilibration of CO and H_2O as material migrated inward to 1 – 2 AU would have returned both CO and H_2O to the bulk isotopic values of the parent cloud. For the model presented here, in which water formation occurs primarily on grain surfaces, concentration of ice-coated dust with $\Delta^{17}O>0$ at the midplane implies grain growth timescales > 10^4 years. Inward migration of ice-rich meter-sized objects may have then delivered ^{17}O and ^{18}O-rich water to the snowline (Cuzzi & Zahnle 2004). Additionally, layered accretion (Gammie 1996) is likely to have been important in the entire self-shielding region of the disk due to surface ionization, with the result that $\Delta^{17}O$-rich H_2O and O_2 (formed by H_2O photolysis) were deposited along the top of the disk dead zone (< 10 AU in the disk model assumed here). Detailed meteoritical analyses can provide constraints on the evolution of $\Delta^{17}O$ in nebular water in the terrestrial planet forming region, as recently demonstrated for CAIs in CR chondrites (Krot et al. 2005).

6. Estimating Initial Gas $\Delta^{17}O$ in the Early Solar Nebula from the Meteorite Record

The isotopic composition of inner nebula gas obtained from the meteorite data can be compared with the predictions of the CO self-shielding model of Lyons & Young (2005) as a check on the veracity of the model. There is considerable meteoritical evidence that the range in $\Delta^{17}O$ among solar system materials arose from exchange between a ^{16}O-poor gas and ^{16}O-rich dust and rock melts (Clayton 1993; Choi *et al.* 1997). Estimates of the original oxygen isotopic composition of the solar nebula gas prior to exchange of oxygen with rock material can be made by assuming that the original solids in the solar system were ^{16}O rich (e.g., Clayton & Mayeda 1984). One then equates the most ^{16}O-rich solids observed with the isotopic composition of the solids prior to exchange.

The mass-dependent oxygen isotope fractionations among phases present in the inner solar nebula are sufficiently small that we can be assured that the initial gas composition is recorded by changes in rock $\delta^{17}O$ and $\delta^{18}O$. The equilibrium isotope

fractionation between condensed phases (solid rock or silicate liquid) and O-bearing gas species is 2‰ or less at temperatures relevant to the early stages of inner solar nebula evolution (T ~ 1500 K) (Onuma et al. 1972), and the fractionation between the major O-bearing gas species themselves, CO and H_2O, is about 2.5‰ at these same temperatures (Onuma et al. 1972). When compared with the ~ 50‰ shifts in both $\delta^{17}O$ and $\delta^{18}O$ that characterize the evolution of rocks in the solar system, these mass-dependent fractionations between solid/liquid rock, H_2O and CO gas in the inner nebula impart deviations to the slope of the line in three-isotope space of at most a few per cent.

Previously, workers used the oxygen isotopic effects of aqueous alteration in carbonaceous chondrites to arrive at estimates of the original nebular gas oxygen isotope ratios (Clayton & Mayeda 1984; Young 2001). These studies arrived at somewhat different results in detail. Establishing the precise initial isotopic composition of the liquid water that reacted with CM chondrites requires a detailed understanding of the geological setting in which the aqueous alteration took place (Young 2002).

Ambiguity surrounding the isotopic composition of liquid water in carbonaceous chondrite parent bodies is sidestepped by recognizing that aqueous alteration is but one of a number of processes that resulted in exchange of oxygen isotopes between the condensed precursor rock phases and the nebular gas phase. The details of these processes are unimportant for defining the end member oxygen isotopic compositions of gas and dust prior to exchange of oxygen. We know, for example, that there were profound changes in $\delta^{17}O$ and $\delta^{18}O$ in the nebula well before aqueous alteration in parent bodies (e.g., differences in $\Delta^{17}O$ among chondrules and CAIs).

All that is required to constrain the original isotopic composition of the inner solar system gas is an estimate of the fraction of oxygen that was bound as rock-forming dust relative to the fraction of oxygen that was in the gas. The relevant mass-balance equation is

$$\delta^{o}_{rx} x^{o}_{rx} + \delta^{o}_{gas} x^{o}_{gas} = \delta^{f}_{rx} x^{f}_{rx} + \delta^{f}_{gas} x^{f}_{gas} \qquad (6)$$

where superscript o refers to the initial condition, superscript f refers to the final condition, δ represents the oxygen isotope ratio of interest in per mil, x_{rx} is the fraction of oxygen bound to rock-forming elements and x_{gas} is the oxygen fraction in the gas phase. If $x^{o}_{rx} = x^{f}_{rx}$ (i.e., the proportion of gas to dust was in steady state) then

$$\delta^{f}_{gas} - \delta^{o}_{gas} = F(\delta^{o}_{rx} - \delta^{f}_{rx}) \qquad (7)$$

where $F=x_{rx}/(1-x_{rx})$ is the number of oxygen atoms present as rock (solid or liquid) divided by the number of atoms present in the gas phase. We will assume that solar relative abundances of the rock-forming elements, oxygen, and carbon apply to the nebula (Anders & Grevesse 1989), taking into account the recent revision of the solar abundance of oxygen from 8.9 to 8.6 dex (Melendez 2004) and carbon from 8.5 dex to 8.4 dex (Allende Prieto et al. 2002). With these values $F = 0.36$. We will assume further that δ^{o}_{rx}, for both $\delta^{17}O$ and $\delta^{18}O$, was -50‰ (Clayton 1993; Clayton 2002), a value that corresponds to the most ^{16}O-rich CAI material. We will also assume that the shifts due to gas-rock exchange were along a slope-1.00 line as indicated by the self shielding calculations in our model and by estimates of the primitive oxygen

mixing line recorded in meteorites (Young & Russell 1998; Young et al. 1999). Changes in $\delta^{17}O$ therefore equal those in $\delta^{18}O$ and changes in both values are expressed succinctly by a change in $\Delta^{17}O$. Based on the oxygen isotopic compositions of Earth, Moon, Mars, and Vesta (assuming Vesta is represented by the HED meteorites), it appears that vast majority of rocky material in the solar system wound up with $\Delta^{17}O$ within 0.3 ‰ of terrestrial. The indicated change in rock-bound $\Delta^{17}O$ is therefore from ~ -24‰ (δ^{o}_{rx}) to 0‰ (δ^{f}_{rx}). With these values equation (2) yields $\delta^{f}_{gas} - \delta^{o}_{gas}$ = - 8.6‰, implying a minimum initial gas $\Delta^{17}O$ of +8.6‰, if gas and rock equilibrated. Deviations in planetary $\delta^{18}O$ from the intersection of the slope-1.0 line and the terrestrial line ($\Delta^{17}O = 0$) can be explained by evaporation in the nebula and by open-system aqueous alteration within parent bodies subsequent to nebular processing.

The calculation above means that if rock $\Delta^{17}O$ increased by 24‰, as seems to be the case, then an 8.6 ‰ decrease in gas $\Delta^{17}O$ is required to balance the effect. Clayton & Mayeda (1984) used a similar calculation, together with the oxygen isotopic shifts associated with aqueous alteration of CM carbonaceous chondrites, to arrive at an initial gas composition of $\delta^{18}O$ = +30‰ and $\delta^{17}O$ = + 24‰, corresponding to $\Delta^{17}O$ = 8.6‰. Although the fact that these estimates match so well is no doubt in part coincidental, it does appear as though the minimum value for gas $\Delta^{17}O$ of ~ 9‰ is a robust result. In detail, the Clayton & Mayeda estimate is on the high-$\delta^{18}O$ extension of the CCAM line defined mainly by CAIs in the Allende meteorite and with a slope of 0.94 in three-isotope space. Young (2001) showed that the same isotopic constraints in the CM chondrites can be satisfied by reaction between rock and an aqueous fluid with an initial composition that lies on the slope-1.0 line in three isotope space (water ice and liquid water are separated by only 3 ‰ at equilibrium, rendering the distinction between liquid and ice negligible in the present context (O'Neil 1968)).

The calculation above can be extended to provide a constraint on the isotopic composition of H_2O in the inner solar nebula for comparison with the predictions of the CO photolysis model. The carrier of high $\Delta^{17}O$ into the inner solar system was water. Thermodynamics and kinetics would have conspired to assure that the most stable oxygen-bearing species in the nebula was CO (Prinn & Fegley 1989; Krot et al. 2000). For this reason, one can estimate the nominal nebular H_2O/CO ratio by assigning all of the oxygen in the gas phase to carbon with the remainder available for formation of H_2O, yielding H_2O/CO = 0.5 for solar abundances of C and O. This represents a minimum for the nebula. In the CO self-shielding hypothesis described here, H_2O/CO in the inner solar nebula should have risen above the baseline value of 0.5 by virtue of preferential transport of H_2O ices incorporated in meter-sized objects inwards through the snowline (Cuzzi & Zahnle 2004). The oxygen mass-balance expression for the gas composed of CO and H_2O is then

$$\delta_{gas} = f_{H2O}\delta^{o}_{H2O} + (1 - f_{H2O})\delta^{o}_{CO} \qquad (8)$$

where f_{H2O} refers to the mixing ratio (oxygen fraction) for water and δ_{gas} is the oxygen isotopic composition of the gas in bulk (allowing for isotopic exchange between CO and H_2O at high T).

The water $\Delta^{17}O$ values implied by equation (3) support the predictions of the CO self shielding model for ^{16}O variability in the inner solar nebula. For f_{H2O} = 0.5, δ^{o}_{CO} = -24‰, as assumed in our model calculations, and δ_{gas} = + 8.6‰ (see above), the water $\Delta^{17}O$ is 41‰. This value is a maximum based on the minimum solar f_{H2O}. Higher mixing ratios result in lower water $\Delta^{17}O$. For example, with f_{H2O} = 0.75, water $\Delta^{17}O$ = 19‰.

There is some evidence for water $\Delta^{17}O$ values greater than ~ 9‰. Young (2001) showed that the $\delta^{17}O$ and $\delta^{18}O$ values of aqueous alteration products in carbonaceous chondrites are reproduced using realistic rates of water-rock reactions and pore water flow if the original water ice had a $\Delta^{17}O$ of ~ 16‰.

That an influx of water into the inner nebula (Cuzzi & Zahnle 2004) could have produced a positive value of $\Delta^{17}O$ is a natural consequence of the CO self shielding model described here (Lyons & Young 2005), as well as the self-shielding model of Yurimoto & Kuramoto (2004). The models also predict that there should be a general correlation between the fugacity of oxygen and $\Delta^{17}O$ in inner solar system materials. To the extent that CAIs, the most ^{16}O-rich objects in the solar system, are also among the most reduced rocks (Krot et al. 2000), the prediction appears to be born out by the data. Production of ^{17}O and ^{18}O-rich water in the outer solar nebula also provides a natural explanation for the correlation between ^{16}O and the refractory nature of some solids. Refractory minerals should have retained their original ^{16}O-rich compositions because they would have had limited opportunity for reaction with gas during their transit through the nebula (either by evaporation and recondensation or by partial melting). That some refractory minerals retain isotope anomalies that cannot be explained by proximity to the nascent star attests to their unreactive nature during their transit through the nebula (Fahey et al. 1987). There is also evidence that CAIs may have condensed out of ^{16}O-rich gas present in the inner solar nebula before the arrival of nebular H_2O isotopically enriched by CO self-shielding (Krot et al. 2002).

7. Conclusions

Based on our 1D photochemical model results (Lyons & Young 2005), we conclude that if CO self-shielding occurred primarily in the solar nebula, a strong FUV source was present (~10^3 times ISM). Such an FUV source is consistent with either a 10^3-fold enhancement in FUV radiation from an early B or O-star at a distance of ~ 1 parsec (i.e., solar birth in an association of ~ 200 stars). Additionally, the 1D model requires vigorous vertical mixing ($\alpha \sim 10^{-2}$) to ensure that a significant fraction of CO is photolyzed, and radial transport inward from ~ 20-30 AU. Inclusion of H_2 absorption effects during CO photodissociation yields nebular water with a $\delta^{17}O/\delta^{18}O$ ratio comparable to CAI measurements.

A key test of the CO self-shielding scenario, regardless of where the self-shielding occurs, is that solar oxygen isotopes are comparable to the lightest CAIs (Clayton 2002). Recent depth profiles of oxygen isotopes in lunar metal grains suggest that the most energetic component of the solar wind does indeed have light oxygen isotopes (Hashizume & Chaussidon 2005). Analysis of GENESIS solar wind samples should provide the most unambiguous test of solar oxygen isotopes. An independent test of CO self-shielding will come from astronomical observations of CO

and H_2O isotopologue ratios by the next generation of infrared and submillimeter telescopes (e.g., ALMA and Herschel).

Acknowledgments. J.R.L. thanks K. McKeegan, J. Cuzzi and A. Boss for discussions, and S. Krot and K. Kuramoto for thoughtful reviews. J.R.L. acknowledges funding from the NASA Origins Program and from the NASA Astrobiology Institute. E.D.Y. acknowledges support from the NASA Astrobiology Institute. IGPP publication No. 6238.

References

Adams, F. C., Hollenbach, D., Laughlin, G., & Gorti, U. 2004, ApJ, 611, 360
Aikawa, Y., & Herbst, E. 2001, A&A, 371, 1107
Aikawa, Y., van Zadelhoff, G. J., van Dishoeck, E. F., & Herbst, E. 2002, A&A, 386, 622
Allende Prieto, C., Lambert, D. L., & Asplund, M. 2002, ApJ, 573, L137
Anders, E., & Grevesse, N. 1989, Geochim. Cosmochim. Acta, 53, 197
Bally, J., & Langer, W. D. 1982, ApJ, 255, 143
Cassen, P., & Moosman, A. 1981, Icarus, 48, 353
Chiang, E. I., & Goldreich, P. 1997, ApJ 490, 368
Chick, K. M., & Cassen, P. 1997, ApJ, 477, 398
Choi, B. G., McKeegan, K. D., Leshin, L. A., & Wasson, J. T. 1997, Earth Planet. Sci. Lett., 146, 337
Choi, B. G., Krot, A. N., McKeegan, K. D., & Wasson, J. T. 1998, Nature, 392, 577
Clayton, D. D. 1988, ApJ, 334, 191
Clayton, R. N. 1993, Ann. Rev. Earth Planet. Sci., 21, 115
Clayton, R. N. 2002, Nature, 415, 860
Clayton, R. N., Grossman, L., & Mayeda, T. K. 1973, Science, 182, 485
Clayton, R. N., Onuma, O., Grossman, L., Mayeda, T. K. 1977, Earth Planet. Sci. Lett., 34, 209
Clayton, R. N., & Mayeda, T. K. 1984, Earth Planet. Sci. Lett., 67, 151
Cuzzi, J. N., Dobrovolskis, A. R., & Hogan, R. C. 1996, in Chondrules and the Protoplanetary Disk, eds. R. H. Hewins, R. H. Jones, & E. R. D. Scott (Cambridge: Cambridge Univ. Press), 35
Cuzzi, J. N., & Zahnle, K. J. 2004, ApJ, 614, 490
D'Alessio, P., Calvet, N., Hartmann, L., Lizano, S., & Canto, J. 1999, ApJ, 527, 893
Fahey, A. J., Goswami, J. N., McKeegan, K. D., & Zinner, E. 1987, Geochim. Cosmochim. Acta, 51, 329
Federman, S. R. et al. 2003, ApJ, 591, 986
Gammie, C. F. 1996, ApJ, 457, 355
Gao, Y. Q., & Marcus, R. A. 2001, Science, 293, 259
Hasegawa, T. I., Herbst, E., & Leung, C. M. 1992, ApJ, 82, 167
Hashizume, K., & Chaussidon, M. 2005, Nature, 434, 619
Imhoff, C. L., & Appenzeller, I. 1987, in Exploring the Universe with the IUE Satellite, ed. Y. Kondo (Dordrecht: Reidel), 295
Kamp, I., & Bertoldi, F. 2000, A&A, 353, 276
Krot, A. N., Fegley, B., Palme, H., & Lodders, K. 2000, in Protostars and Planets IV. eds. V. Mannings, A. P. Boss, & S. S. Russell (Tucson: Univ. Arizona Press), 1019
Krot, A. N. et al. 2002, Science, 295, 1051
Krot, A. N. et al. 2005, ApJ, 622, 1333
Lee, H. H., Herbst, E., Pineau des Forêts, G., Roueff, E., & Le Bourlot, J. 1996, A&A, 311, 690

Le Teuff, Y. H., Millar, T. J., & Markwick, A. J. 2000, A&AS, 146, 167
Lunine, J. I., Engel, S., Rizk, B., & Horanyi, M. 1991, Icarus, 94, 333
Lyons, J. R. 2002, Astrobiology, 2, 532
Lyons, J. R., & Young, E. D. 2003, Lunar Planet. Sci., 34, 1981
Lyons, J. R., & Young, E. D. 2004, Lunar Planet. Sci., 35, 1970
Lyons, J. R., & Young, E. D. 2005, Nature, 435, 317
Marcus, R. A. 2004, J. Chem. Phys., 121, 8201
Maréchal, P., Viala, Y. P., Pagani, L. 1997, A&A, 328, 617
Markwick, A. J., Ilgner, M., Millar, T. J., & Henning, Th. 2002, A&A, 385, 632
Matsuhisa, Y., Goldsmith, J. R., Clayton, R. N. 1978, Geochim. Cosmochim. Acta, 42, 173
McCandliss, S. R. 2003, PASP, 115, 65
McKeegan, K. D., & Leshin, L. A. 2001, in Stable Isotope Geochemistry, Reviews in Mineralogy and Geochemistry, 43, eds. Valley, J. W., & Cole, D. R. (Washington DC: Mineral. Soc. America), 279
Melendez, J. 2004, ApJ, 615, 1042
Navon, O., & Wasserburg, G. J. 1985, Earth Planet. Sci. Lett., 73, 1
Neufeld, D. A., & Hollenbach, D. J. 1994, ApJ, 428, 170
O'Neil, J. R. 1968, J. Chem. Phys., 72, 3683
Onuma, N., Clayton, R. N., & Mayeda, T. K. 1972, Geochim. Cosmochim. Acta, 36, 169
Prinn, R. G. 1990, ApJ, 348, 725
Prinn, R. G., & Fegley, B. 1989, in Origin and Evolution of Planetary Satellite Atmospheres, eds. S. K. Atreya, J. B. Pollack, & M. S. Matthews (Tucson: Univ. Arizona Press), 78
Sheffer, Y., Lambert, D. L., & Federman, S. R. 2002, ApJ, 574, L171
Stevenson, D. J. 1990, ApJ, 348, 730
Stone, J. M., Gammie, C. F., Balbus, S. A., & Hawley, J. F. 2000, in Protostars and Planets IV, eds. Manning, V., Boss, A. P., & Russell, S. S. (Tucson: Univ. Arizona Press), 589
Thiemens, M. H., & Heidenreich, H. E. 1983, Science, 219, 1073
van Dishoeck, E. F., & Black, J. H. 1988, ApJ, 334, 771
van Zadelhoff, G. J., Aikawa, Y., Hogerheijde, M. R., & van Dishoeck, E. F. 2003, A&A, 397, 789
Willacy, K., Klahr, H. H., Millar, T. J., & Henning, Th. 1998, A&A, 338, 995
Wurm, G., & Blum, J. 1998, Icarus, 312, 125
Young, E. D. 2001, Phil. Trans. R. Soc. Lond. A., 359, 2095
Young, E. D. 2002, Meteorit. Planet. Sci., 37 Suppl., A153
Young, E. D., & Russell, S. S. 1998, Science, 282, 452
Young, E. D., Ash, R. D., England, P., & Rumble, D. III. 1999, Science, 286, 1331
Young, E. D., & Lyons, J. R. 2003, Lunar Planet. Sci., 34, 1923
Yurimoto, H., & Kuramoto, K. 2004, Science, 305, 1763